Effects of Nb-Alloying on High-Temperature Oxidation of MoSi₂

A.A. Sharif

California State University Los Angeles, Department of Mechanical Engineering

5151 State University Dr., Los Angeles, CA 90032-8153, USA

The effects of alloying with 0.5, 1.0, and 2.0 at.% Nb on oxidation resistance of MoSi₂ are investigated at temperature range of 1400 °C–1700 °C. Rapid formation of a stable protective layer of silica resulted in a parabolic oxidation rate. The oxide layer thickness and the sample weight increased with increasing oxidation time. Impurities accelerated oxidation rate of MoSi₂ only slightly, however, did not affect the rate controlling mechanism for oxidation. There was no correlation between oxidation rate and the amount of impurity. The values of activation energies for oxidation of pure MoSi₂ and Nb-alloyed samples were similar to activation energy for diffusion of O₂ through silica. Diffusion of O₂ through the oxide scale remained the rate controlling mechanism with or without Nb impurity.

1. Introduction

Molybdenum disilicide (MoSi₂) has superb oxidation resistance up to 1700 °C, which makes it a great candidate for applications requiring high-temperature stability. Development of MoSi₂-based alloys as ultrahigh-temperature structural materials to improve on operating temperature of Ni-based super alloys have been the focus of many investigations in the past two decades [1, 2]. Elevating the operating temperature of gas engines above the operating temperature of superalloys would result in significant increase in efficiency, considerable cost savings, and reduction of environmentally harmful emissions. However, there are some inherent problems with the use of MoSi₂-based alloys as structural materials. MoSi₂ transitions from brittle to ductile are only at high temperatures ($\approx$ 900 °C); it undergoes pest oxidation at temperature range of $\approx$ 500–800 °C; and it has inadequate strength at elevated temperatures. Various alloying approaches have proven successful in eliminating some of the problems with application of MoSi₂-based alloys as structural materials. It was shown that alloying and eliminating porosity may hinder the pest oxidation problem of MoSi₂ [3, 4]. Furthermore, ceramic reinforcements such as SiC, Si₃N₄, WSi₂, or NbSi₂ improve its mechanical properties at high temperatures [5–7].

Investigations on alloying MoSi₂ with low fraction of impurities while keeping the body-centered tetragonal ($C11_b$) structure of MoSi₂ have been more promising. First principles calculations have predicted enhancement in ductility of MoSi₂ by substitutional alloying of V and Nb for Mo and Mg and Al for Si [8]. Experimentally, unusually high strengthening was observed by substitutional Re alloying of MoSi₂ [9] and concurrent low-temperature softening and high-temperature strengthening was obtained by alloying with Al or Nb within their solubility limit in MoSi₂ [10–14]. Nb was found to be the most potent alloying element in improving mechanical

properties of MoSi₂. Addition of 1 at.% Nb to MoSi₂ was found to lower its brittle-to-ductile transition temperature to room temperature [10]. At very high temperatures ($\approx$ 1600 °C), alloying MoSi₂ with 1 at.% Nb increased its yield strength by an order of magnitude compared to pure samples [10]. These alloying strategies may only be utilized successfully if the impurities do not affect oxidation resistance of MoSi₂ adversely. Therefore, studies on oxidation resistance should be conducted parallel with investigations on the effects of impurities on mechanical properties of MoSi₂.

Outstanding oxidation resistance of MoSi₂ above its pesting temperature up to 1700 °C results from the formation of a protective silica (SiO₂) layer [15], typical of all SiO₂-forming materials. In these materials, SiO₂ acts as a barrier against further oxidation [16]. Above the pest oxidation temperature, oxidation behavior of MoSi₂ is identical to that of Si up to 1400 °C [17]. The kinetics of growth of SiO₂ layer on MoSi₂ is governed by three processes: (1) transport of the oxidizing species for absorption, (2) diffusion of the oxidant through the oxide layer, and (3) oxidant reaction with the bulk MoSi₂ to form SiO₂. The solution for the kinetic equations results in a short linear region expressed by [16]:

$$x = k_l(t + \tau), \tag{1}$$

followed by a long parabolic region described by

$$x^2 = k_p t, \tag{2}$$

where x is the oxide thickness at time t, τ is the transition time from linear to parabolic oxidation relations, and k_l and k_p are the linear and parabolic oxidation rate constants, respectively. The linear rate is due to interfacial reaction-controlled mechanism at short times and parabolic regime is the result of diffusion-controlled mechanism at longer times.

Complexities in the kinetics of oxidation of MoSi₂ arise from formation of other Mo–Si phases as well as phase transformations in SiO₂ scale. Local consumption of Si

may result in formation of Mo_5Si_3 at low or high temperatures [18–21] but Mo_3Si has been observed to result from the reaction of Mo_5Si_3 with O_2 only at low temperatures [22]. At high temperatures, upon rapid formation of a stable oxide layer, Mo_5Si_3, which forms beneath the oxide scale, is insulated from oxygen and formation of Mo_3Si is prevented. Finally, since scale growth is a diffusion-controlled process, the extent of crystallization of SiO_2, may affect diffusion rate and, consequently, oxidation mechanism. Nb seems to be the most potent alloying element for improving mechanical properties of $MoSi_2$ concurrently at low- and high-temperatures.

The present work investigates the effects of Nb impurities (2 at.%), on oxidation resistance of $MoSi_2$ at the target application temperatures of the alloy with a focus on developing an $MoSi_2$-based alloy that exhibits low--temperature ductility and enhanced high-temperature strength while retaining and inherently superb oxidation resistance of $MoSi_2$.

2. Experimental procedure

Polycrystalline unalloyed $MoSi_2$ and $(Mo_{1-x}, Nb_x)Si_2$ buttons with $x = 0.015$, 0.03, and 0.06 for 0.5, 1.0, and 2.0 at.% Nb, respectively, were prepared by arc-melting elemental high purity Mo, Si, and Nb in an argon atmosphere. Following the results of previous investigations, excess Si was used to compensate for Si loss that occurs during arc-melting [13]. The starting composition of the alloys were $MoSi_{2.01}$ and $(Mo_{1-x}, Nb_x)Si_{2.01}$. Experimental procedure is detailed in previous publications [10, 23, 24].

3. Results and discussion

Cross-sections of $MoSi_2$ samples containing (a) 0.0, (b) 0.5, (c) 1.0, and (d) 2.0 at.% Nb after oxidation for 100 h at 1700 °C are shown in Fig. 1. It should be noted that
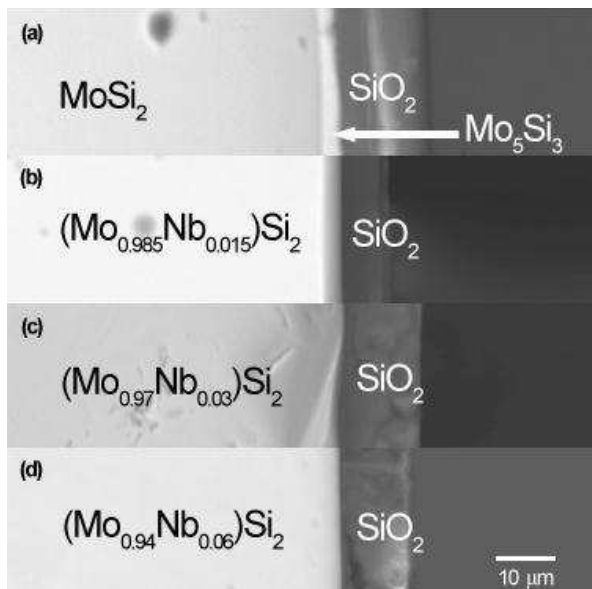
Fig. 1. Comparison of the cross-sections of the oxide scales for all alloys after 100 h oxidation at 1700 °C.
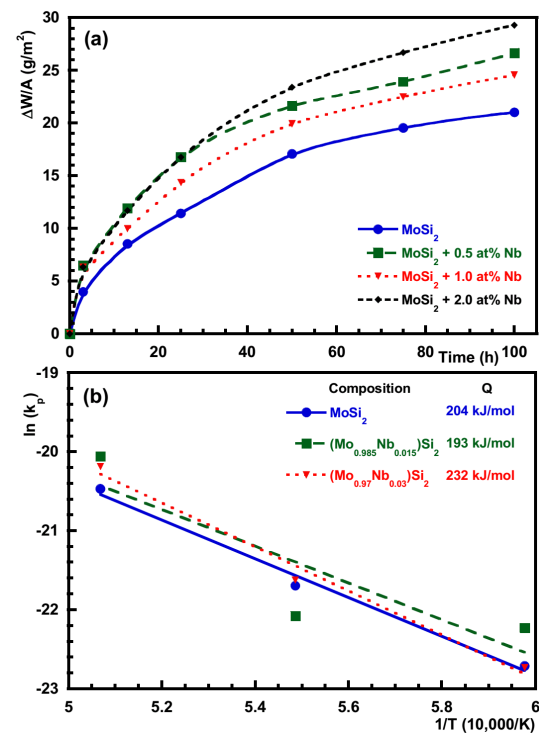
Fig. 2. (a) Results of isothermal oxidation of unalloyed $MoSi_2$ and samples containing Nb at 1700 °C. (b) Plots of inverse temperature vs. logarithmic parabolic rate constant for calculating activation energy for oxidation. Values of Q for each composition are listed next to the legend.

there was some variation in the oxide thickness from one point on the sample to the next point. The main difference distinguishing oxidation of pure sample from those containing Nb was the presence of Mo_5Si_3 layer in unalloyed samples. Formation of Mo_5Si_3 has been reported previously as a byproduct of rapid consumption of Si at the scale/bulk interface at elevated temperatures [23]. Mo_5Si_3 was not observed in any Nb-containing sample during investigations reported here. Presence of Nb impurity could prevent Mo_5Si_3 formation if it lowered the oxidation rate of $MoSi_2$, which would allow for diffusion of Mo from Si-starved oxide interface to lower concentrations at the center of the sample.

However, as seen in Fig. 2a, at 1700 °C Nb impurity enhanced the oxidation rate of $MoSi_2$. Another mechanism for prevention of Mo_5Si_3 formation could be enhanced solubility of Mo in the $MoSi_2$ matrix due to Nb impurity. Nb-rich regions were observed in all Nb-containing samples after oxidation at 1700 °C for 100 h. Energy dispersive X-ray spectroscopy (EDS) analysis of these regions in 2 at.% Nb-containing samples indicated 41.4, 40.2, and 18.4 at.% Mo, Si, and Nb, respectively. These values correspond to a 3/2 atomic ratio of $((9/13)Mo+(4/13)Nb)/Si$ or $((9/13)Mo+(4/13)Nb)_3Si_2$. Mo_3Si_2 and Nb_3Si_2 are metastable phase of Mo–Si and Nb–Si systems, respectively [25, 26]. These regions remained scattered in the $MoSi_2$ matrix thus a Si-deficient phase did

not form in Nb-containing samples beneath the oxide layer as it did in pure MoSi$_2$. The fraction of $((9/13)\text{Mo}+(4/13)\text{Nb})_3\text{Si}_2$ phase increased with Nb content but remained distributed along the grain boundaries in all samples.

The parabolic oxidation rate constants at three test temperatures were calculated from the slope of the plot of time (t) vs. change in specific weight squared $(\Delta W/A)^2$ as described by Eq. (2). Using the Arrhenius relation

$$k_\text{p} = k_0 \exp\left(-\frac{Q}{RT}\right) \qquad (3)$$

for thermally activated oxidation process, the value of activation energy for oxidation (Q) may be calculated from the slope of the line obtained from plot of $1/T$ vs. $\ln(k_\text{p})$. The Arrhenius lines for these calculations are shown in Fig. 2b.

The values of k_p and Q are listed in Table for all samples at 1400 °C, 1550 °C, and 1700 °C except for 2 at.% Nb containing alloy at 1400 °C due to sample failure. Therefore, neither k_p at 1400 °C nor Q could be calculated for this alloy. Activation energies of 193 and 232 kJ/mol were calculated for 0.5 and 1.0 at.% Nb containing samples, respectively. Comparing the value of Q for unalloyed sample, 204 kJ/mol, it is clear that Nb impurity at the level used here, does not alter the rate controlling mechanism for oxidation of MoSi$_2$. The values of activation energies calculated here are within the range of values of activation energy for diffusion of molecular oxygen (O$_2$) through vitreous silica [27]. Therefore, diffusion of O$_2$ through the oxide scale is the rate controlling mechanism for oxidation.

Calculated values of parabolic oxidation rate constants (k_p) and activation energies for oxidation (Q).   TABLE

Alloy	k_p (1400 °C)	k_p (1550 °C)	k_p (1700 °C)	Q [kJ/mol]
MoSi$_2$	1.37×10^{-10}	3.78×10^{-10}	1.29×10^{-9}	204
(Mo$_{0.985}$,Nb$_{0.015}$)Si$_2$	2.21×10^{-10}	2.59×10^{-10}	1.96×10^{-9}	194
(Mo$_{0.97}$,Nb$_{0.03}$)Si$_2$	1.34×10^{-10}	4.06×10^{-10}	1.71×10^{-9}	232
(Mo$_{0.94}$,Nb$_{0.06}$)Si$_2$	–	1.69×10^{-9}	2.44×10^{-9}	–

Degree of crystallinity of silica would affect the diffusion rate of O$_2$. EDS elemental mapping did not show detectable concentration of Nb in the silica scale. Therefore, this study could not attribute any change in oxidation behavior of MoSi$_2$ to effects of Nb on crystallization of SiO$_2$.

Finally, oxidation rate of Nb-containing samples, as shown in Fig. 2a, increased from 1.0 at.% to 2.0 at.% Nb impurity. Although Nb impurity enhanced the rate of oxidation slightly, its effect did not depend on the impurity concentration. The presence of an Mo$_5$Si$_3$ layer beneath the oxide scale may abate the oxidation rate by creating another barrier for diffusion of Si to reach the scale/matrix interface. The increase in the rate of oxidation in the samples containing Nb impurity may be due to elimination of Mo$_5$Si$_3$ diffusion barrier in the presence of Nb.

4. Conclusions

Alloying of MoSi$_2$ by 0.5, 1.0, and 2.0 at.% Nb did not result in significant deterioration of oxidation resistance of the alloy. Diffusion of O$_2$ through the oxide layer remained the rate controlling mechanism with or without Nb impurity. Since previous investigations have shown that minor Nb alloying produces significant improvements in mechanical properties of MoSi$_2$, herein, it is concluded that Nb-alloying may be the path towards

developing a viable MoSi$_2$-based alloy with ambient temperature ductility, high strengths at ultrahigh temperatures, and excellent oxidation resistance up to 1700 °C.

References

[1] A.K. Vasudevan, J.J. Petrovic, *Mater. Sci. Eng. A* **155**, 1 (1992).

[2] J.J. Petrovic, *Ceram. Eng. Sci. Proc.* **18**, 3 (1997).

[3] M.G. Hebsur, M.V. Nathal, *Structural Intermetallics*, The Minerals, Metals and Materials Society, Warrendale (PA) 1997, p. 949.

[4] K. Kurokawa, H. Houzumi, I. Saeki, H. Takahashi, *Mater. Sci. Eng. A* **261**, 292 (1999).

[5] S. Bose, *Mater. Sci. Eng. A* **155**, 217 (1992).

[6] H. Inui, T. Nakamoto, K. Ishikawa, M. Yamaguchi, *Mater. Sci. Eng. A* **261**, 131 (1999).

[7] Y. Umakoshi, T. Nakano, K. Kishimoto, D. Furuta, K. Hagihara, M. Azuma, *Mater. Sci. Eng. A* **261**, 113 (1999).

[8] U.V. Waghmare, E. Kaxiras, V.V. Bulatov, M.S. Duesbery, *Modeling Simul. Mater. Sci. Eng.* **6**, 493 (1998).

[9] A. Misra, A.A. Sharif, J.J. Petrovic, T.E. Mitchell, *Acta Mater.* **48**, 925 (2000).

[10] A.A. Sharif, A. Misra, T.E. Mitchell, *Mater. Sci. Eng. A* **358**, 289 (2003).

[11] A.A. Sharif, J.J. Petrovic, A. Misra, T.E. Mitchell, in: *Annual Meeting of the American Ceramic Society*, Eds.: J.P. Singh, N.P. Bansal, A. Bandyopadhyay, American Ceramic Society, Philadelphia 2000, p. 69.

[12] A.A. Sharif, A. Misra, J.J. Petrovic, T.E. Mitchell, *Scr. Mater.* **44**, 879 (2001).

[13] A.A. Sharif, A. Misra, J.J. Petrovic, T.E. Mitchell, *Intermetallics* **9**, 869 (2001).

[14] A.A. Sharif, A. Misra, T.E. Mitchell, *Scr. Mater.* **52**, 399 (2005).

[15] J. Schlichting, *Mater. Chem.* **4**, 93 (1979).

[16] B.E. Deal, A.S. Grove, *J. Appl. Phys.* **36**, 3770 (1965).

[17] H.J. Grabke, G.H. Meier, *Oxid. Metals* **44**, 147 (1995).

[18] K. Ito, T. Hayashi, M. Yokobayashi, H. Numakura, *Intermetallics* **12**, 407 (2004).

[19] Y.T. Zhu, M. Stan, S.D. Conzone, D.P. Butt, *J. Am. Ceram. Soc.* **82**, 2785 (1999).

[20] C.D. Wirkus, D.R. Wilder, *J. Am. Ceram. Soc.* **49**, 173 (1966).

[21] J.B. Berkowitz-Mattuk, R.R. Dils, *J. Electrochem. Soc.* **112**, 583 (1965).

[22] K. Natesan, S.C. Deevi, *Intermetallics* **8**, 1147 (2000).

[23] A.A. Sharif, *J. Mater. Sci.* **45**, 865 (2010).

[24] A.A. Sharif, *J. Alloys Comp.* **518**, 22 (2012).

[25] N. Ponweiser, W. Paschinger, A. Ritscher, J.C. Schuster, K.W. Richter, *Intermetallics* **19**, 409 (2011).

[26] M. Li, L. Song, J. Le, X. Zhang, B. Pei, X. Hu, *Mater. Trans.* **45**, 2785 (2004).

[27] M.L.F. Nascimento, E.D. Zanotto, *Phys. Chem. Glasses: Eur. J. Glass Sci. Technol. B* **48**, 201 (2007).